Düzce Üniversitesi
Teknik Bilimler Dergisi

Duzce University
Journal of Technical Sciences

https://dergipark.org.tr/tr/pub/duted

Research Article

Fe_3O_4/su ile Doldurulmuş Kanatlı Soğutucunun Termodinamik Tersinirlik Açısından Parametrik Analizi

*Hayati Kadir Pazarlioglu[a]**

[a]University of Stuttgart, Institute of Aerospace Thermodynamics, Stuttgart, Germany
* **Sorumlu Yazar:** hayati-kadir.pazarlioglu@itlr.uni-stuttgart.de

ÖZET

Elektronik bir cihazda aşırı yüklenen ısının tatmin edici bir şekilde dağıtılması verimli bir soğutma sistemine bağlıdır. Bu noktada mühendisler ve araştırmacılar, güvenilir çalışma davranışları ve dayanıklılıkları nedeniyle bir ısı kuyusu kullanmayı tercih ederler. Soğutucunun akışkan karakteristiğini ve ısıl performansını artırmak basittir çünkü tasarımındaki herhangi bir küçük değişiklik, hidrotermal özelliklerinde bir artışın yolunu açar. Burada, ferronanoakışkan (Fe_3O_4/su; φ=%2) akan farklı kanatlı (dairesel, kare ve altıgen) ısı kuyularının termo-hidrolik performansını araştırmak için laminer rejim (1000≤Re≤2000) altında parametrik sayısal çalışmalar yapılmıştır. Genel olarak, temel duruma göre en yüksek başarı rakamı (FOM), nanoakışkansız ısı kuyusunda kare kanat tipi kullanılarak Re=1500'de gözlenirken, aynı geometrik konfigürasyonda en düşük toplam entropi üretimi ve en yüksek konvektifisı transferi performansı Re=2000 ve φ=%2'de sergilendi. Ayrıca, nanoakışkanla doldurulmuş ısı kuyusunda kare kanat tipi kullanımının Re=2000'de ortalama Nusselt sayısını (Nu) baz duruma göre %18,41 artırdığı ve aynı karşılaştırma için basınç düşüşünü %59 civarında artırdığı sonucuna varılmıştır. Son olarak, Re=2000 ve φ=%2'de kare kanatlı tip ısı kuyusu kullanılarak toplam entropi üretiminin baz duruma göre %7,71 oranında azaldığı görüldü.

Anahtar Kelimeler: *Entropi Üretimi, Fe_3O_4/su, Isı Kuyusu, İğne Kanatçık, Taşınım Isı Transferi.*

Parametric Analyses of Finned Heatsink Filled with Fe_3O_4/water Regarding Thermodynamic Irreversibility

ABSTRACT

Satisfactory distribution of the over loaded heat in an electronic device depends on an efficient cooling system. In this point, engineers and researchers prefer using a heatsink due to their reliable operation behaviour and durability. To enhance fluid characteristic and thermal performance of the heatsink is simple since any small change in its design paves the way for an increase in its hydrothermal characteristics. Herein, parametric numerical studies were performed under laminar regime (1000≤Re≤2000) to investigate thermo-hydraulic performance of the different finned (circular, square, and hexagonal) heatsinks flowing ferro-nanofluid (Fe_3O_4/water; φ=2%). Overall, the highest figure of merit (FOM) over base case were observed at Re=1500 by utilizing square fin type in the heatsink without nanofluid whilst the lowest total entropy generation and the highest convective heat transfer performance were exhibited at the same geometric configuration at Re=2000 and φ=2%. Besides, it was concluded that the use of square fin type in the heatsink filled with nanofluid augmented average Nusselt number (Nu) by 18.41% compared with base case at Re=2000 and increased pressure drop around 59% for the same comparison. Finally, it was seen that total entropy generation by using square fin type heatsink at Re=2000 and φ=2% was decreased by 7.71% over base case.

Anahtar Kelimeler: *Convective Heat Transfer, Entropy Generation, Fe_3O_4/water, Heatsink, Pin Fin.*

I. INTRODUCTION

Since electronic devices are becoming smaller, their operating temperature is rising, so their operational temperature and accumulating heat over them should safely be distributed to environment (Algburi et al., 2021). Generally, safety running temperature of electronic devices are considered around 85ºC. Therefore, to keep lower than this temperature is essential for any electronic devices (Shahsavar et al., 2021a; Shahsavar et al., 2022a). In this point, heatsinks are usually preferred removing heat from electronic equipment. A period of twenty years, combination of the water and nanoparticles has a great power as a working fluid due to their prestigious thermal properties compared to other conventional working fluids (Pazarlıoğlu et al., 2023a; Pazarlıoğlu et al., 2023b). Furthermore, extended surfaces have a great advantage due to their vivid characteristics on enhancement of the heat transfer rate (Gürsoy et al., 2023; Pazarlıoğlu et al., 2021). In this regard, the use of pin fins present opportunity for researchers and engineers due to their high hydrodynamic behaviour compared to other extended surface types (Ateş et al., 2023; Chen et al., 2020). Next, as can be seen from the literature, low pressure drop and high convective heat transfer rate can be obtained by using pin fin, which leads to higher FOM (Figure of Merit) which is one of the most important parameters for RIC (Research, Investigation, and Commercialization) (Ateş et al., 2022; Pazarlıoğlu et al., 2022a). Parlak et al. (Parlak et al., 2022) have experimentally and numerically investigated micro heatsink with high aspect ratio to optimize it to reach an efficient geometric design parameter. After completion numerical studies, optimum channel height was found as 2 mm. Also, experimental studies showed very good agreement with numerical data obtained from CFD results. Shahsavar et al. (Shahsavar et al., 2022b) numerically performed parametric analyses using silver/water nanofluid under turbulent flow regime. Then, rifled inlet section was used to observe its hydrothermal augmentation. As a result of the study, rifled inlet section has increased FOM considerably. Shahsavar et al. (Shahsavar et al., 2023) was analysed a heatsink filled with nanofluid and applied surface vibration for enhancement of the heat transfer rate. Analyses were performed under laminar regime while the surface vibration method to enhance heat transfer was applied for the first time on a heatsink. It is reported that the use of surface vibration is the effective method for the heat transfer enhancement. Ghazizade-Ahsaee et al. (Ghazizade-Ahsaee et al., 2023) numerically investigated a heatsink analyses for observation of the effect of the inlet velocity profiles under laminar regime. It is reported that the use of non-uniform velocity profile was led to obtaining higher FOM than uniform velocity profile.

Based on the literature review, the use of the different shape of pin fins on heatsink (circular, rectangular, and hexagonal) are rather scarce that is why the use of these type of pin fins in heatsink under laminar flow regime are decided to observe thermal and fluid characteristics and investigate total entropy generation of the proposed system. To the best author knowledge, investigating different fin shapes have a crucial effect for the mass production companies since adding a fin to the system will lead to increase in pressure drop which is not desired effect in the system (Li et al., 2011). Therefore, defining a good fin shape presenting lower pressure drop compared to others will be beneficial for such systems. Besides, the mass production machines are loaded with high thermal residuals during production process. To remove this unneeded effect using a well-designed heatsink enhanced by well-structured pin fins has a considerable effect. In this study, to define therefore the optimum fin geometry for heatsinks which is great opportunity for removing heat from electronic devices will be highlighted, and these outputs will shed light on the literature to understand what types of pin fins are better to use such a system.

II. MATERIAL AND METHOD

Fig. 1. presents geometrical information about proposed heatsink. In this study, ANSYS Fluent 2020 R2 using Finite Volume Method to discretization of governing equations were used to numerically investigate proposed geometry and parametric inputs. The uniform heat flux of q" =80000 W/m^2 for bottom side and non-uniform velocity profile for inlet section were conducted on the heatsink while other walls were kept as adiabatic boundary conditions. Also, no-slip boundary conditions were selected for all geometry's wall, and pressure outlet boundary conditions were applied for the outlet section. Then, the

parametric studies were performed under laminar flow regime taking into account steady-state conditions, single phase approach, and Newtonian fluid. The thermal properties of working fluids can be seen from Table 1.

Table 1. Thermo-physical properties of water and Fe_3O_4 at T=300 K (Tekir et al., 2022).

	Water	Fe_3O_4	Fe_3O_4/water & φ=2%
ρ [kg/m^3]	998	5180	1083
cp [J/kg.K]	4182	670	4122
k [W/m.K]	0.598	80.4	0.6186
μ [Pa.s]	1e-03	-	1.26e-03

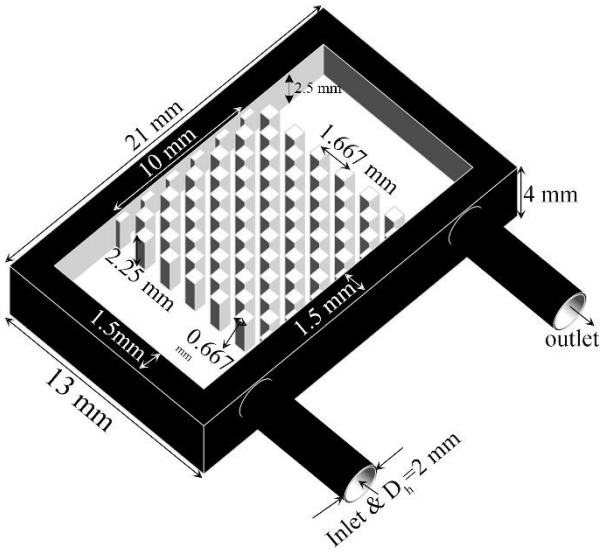

Fig. 1. Dimensions of proposed heatsink.

Then, the definition of the cases was named according to following information; circular pin finned heatsink: Case 1, square pin finned heatsink: Case 2, and hexagon pin finned heatsink: Case 3. It is noted that Case 1 & water is the base case for this study. Moreover, the governing equations (continuity, momentum, and energy) was discretised to observe hydrothermal characteristics of the proposed system.

Continuity (Kays et al., 2004) :

$$\nabla.\vec{V} = 0 \tag{1}$$

Momentum (Kays et al., 2004) :

$$\rho\left(\left(\vec{V}.\nabla\right)\vec{V}\right) = -\nabla P + \rho\vec{g} + \mu\nabla^2\vec{V} \tag{2}$$

Energy (Kays et al., 2004) :

For fluid: $$\rho c_p\left(\left(\vec{V}.\nabla\right)\vec{T}\right) = k_f\nabla^2\vec{V} \tag{3}$$

For solid: $$k_s\nabla^2\vec{V} = 0 \tag{4}$$

After solving these governing equations, these findings should be converted meaningful numbers, so following formulations can be used for this regard:

Reynolds number (Re) (Jiji, 2009):

$$\mathrm{Re} = \frac{\rho V_{avg.} D_h}{\mu} \tag{5}$$

Convective heat transfer coefficient (h) (Jiji, 2009):

$$h = \frac{q''}{T_{CPU_{avg.}} - T_{bulk}} \tag{6}$$

Average Nusselt number (Nu) (Jiji, 2009):

$$Nu = \frac{hD_h}{k} \tag{7}$$

Temperature uniformity (θ) (Shahsavar et al., 2021a):

$$\theta = \frac{T_{CPU_{max}} - T_{CPU_{\min}}}{q''} \tag{8}$$

Thermal resistance (R) (Shahsavar et al., 2021b):

$$R = \frac{T_{CPU_{avg.}} - T_{in}}{q''} \tag{9}$$

Figure of merit (FOM) (Pazarlıoğlu et al., 2022b)

$$FOM = \frac{h_{enhanced} / h_{base}}{\left(\Delta P_{enhanced} / \Delta P_{base}\right)^{1/3}} \tag{10}$$

Thermodynamic irreversibility can be calculated by using below equations (Shahsavar et al., 2021b):

$$\dot{S}'''_{ff} = \frac{\mu}{T}\left\{\begin{array}{l} 2\left[\left(\frac{\partial u}{\partial x}\right)^2 + \left(\frac{\partial v}{\partial y}\right)^2 + \left(\frac{\partial w}{\partial z}\right)^2\right] + \left(\frac{\partial u}{\partial y} + \frac{\partial v}{\partial x}\right)^2 \\ + \left(\frac{\partial u}{\partial z} + \frac{\partial w}{\partial x}\right)^2 + \left(\frac{\partial w}{\partial y} + \frac{\partial v}{\partial z}\right)^2 \end{array}\right\}$$

$$\dot{S}_{ff} = \iiint \dot{S}'''_{ff} dV$$

$$\dot{S}'''_{th} = \frac{k}{T^2}\left(\left(\frac{\partial T}{\partial x}\right)^2 + \left(\frac{\partial T}{\partial y}\right)^2 + \left(\frac{\partial T}{\partial z}\right)^2\right)$$

$$\dot{S}_{th} = \iiint \dot{S}'''_{th} dV$$

$$\dot{S}_{total} = \dot{S}_{ff} + \dot{S}_{th}$$

$$Be = \dot{S}_{th} / \dot{S}_{total} \tag{11}$$

To solve mentioned above governing equations correctly, the most important parameter in finite volume analyses is to create well mesh distribution on geometry. In this study, five different mesh structure were applied on geometry to obtain optimum mesh structure over the body. In the mesh independency studies, the denser mesh should be carried out which region is the most important to observe hydrothermal behaviour of it whereas the other region can be meshed less than important region to take an advantage in terms of computational time. In this study, the denser mesh structure was conducted for finned region, heated surface, inlet, and outlet section due to having high priority for designing a heatsink. While the mesh convergency study can be seen from Table 2, the decided mesh structure (M3) can be seen from Fig. 2.

Table 2. Mesh independency study at Re=2000 for Case 2.

Mesh No	M1	M2	M3	M4	M5
Node	798901	1487976	2687954	3543013	4145810
Nu	42.3	48.87	50.36	50.45	50.30

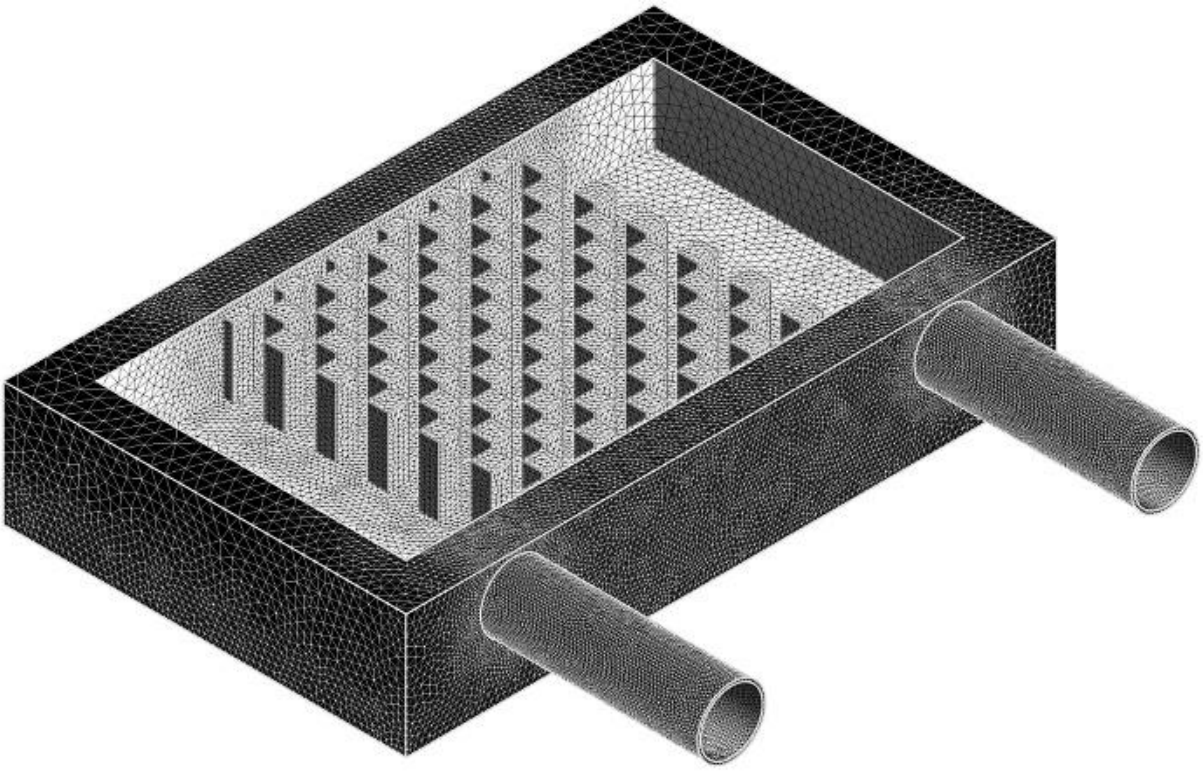

Fig. 2. Mesh structure on heatsink (Case 2).

Before starting analyses of the prosed system, the verification study with the literature should be performed. Therefore, this numerical study was compared with Shahsavar's study (Shahsavar et al., 2021a). This verification can be seen from Table 3.

Table 3. Verification study with a study published in the literature.

Re	Present Study	(Shahsavar et al., 2021a)	Deviation rate (%)
-	Tcpu [K]	Tcpu [K]	-
1000	308.301	307.4	0.293103448
1500	306.944	307.1	0.050797786
2000	306.127	306.7	0.186827519

III. RESULTS

In this section, thermal characteristics and hydraulic behaviour of the finned heatsink have widely been discussed under different circumstances. Fig. 3(a) depicts Nu values for different cases and working fluids under laminar flow conditions. While Case 3&water presented the lowest Nu, Case 2&NF showed the highest Nu for all Re. Especially, the highest rising ratio has been achieved at Re=2000 for Case 2&NF. It is noted that working fluid can be moved around square fins due to wider surface area than other fin types that is why the highest Nu is obtained for this case. Also, this finding is consistency with the study of (Shahsavar et al., 2021a). Pressure drop distribution for different cases can be seen in Fig. 3(b). As can be seen from this figure, the minimum pressure drop value has been faced for Case 1&water at Re=1000 whilst the maximum one has been obtained for Case 3&NF at Re=2000. Case 3 has the widest surface area compared to other cases, so this phenomenon leads to an increase in pressure drop dramatically. Then, using of nanofluid as a working fluid may lead to increase in pressure drop value (Tekir et al., 2022). Fig. 3(c) explains temperature uniformity in terms of different cases and working fluids under same boundary conditions. It can be seen that temperature uniformity decreases as Re increases due to diminishing the temperature of heatsink. Especially, the lowest temperature uniformity is obtained at Re=2000 due to hitting the bottom in terms of temperature of heatsink. Fig. 3(d) shows thermal resistance of finned heatsink for all cases at different Re. While the highest thermal resistance is obtained for Case 1&water,

the lowest thermal resistance is handled for Case 2&NF. Case 2&NF presents a better approach for thermal resistance due to effective cooling for finned heatsink for all Re.

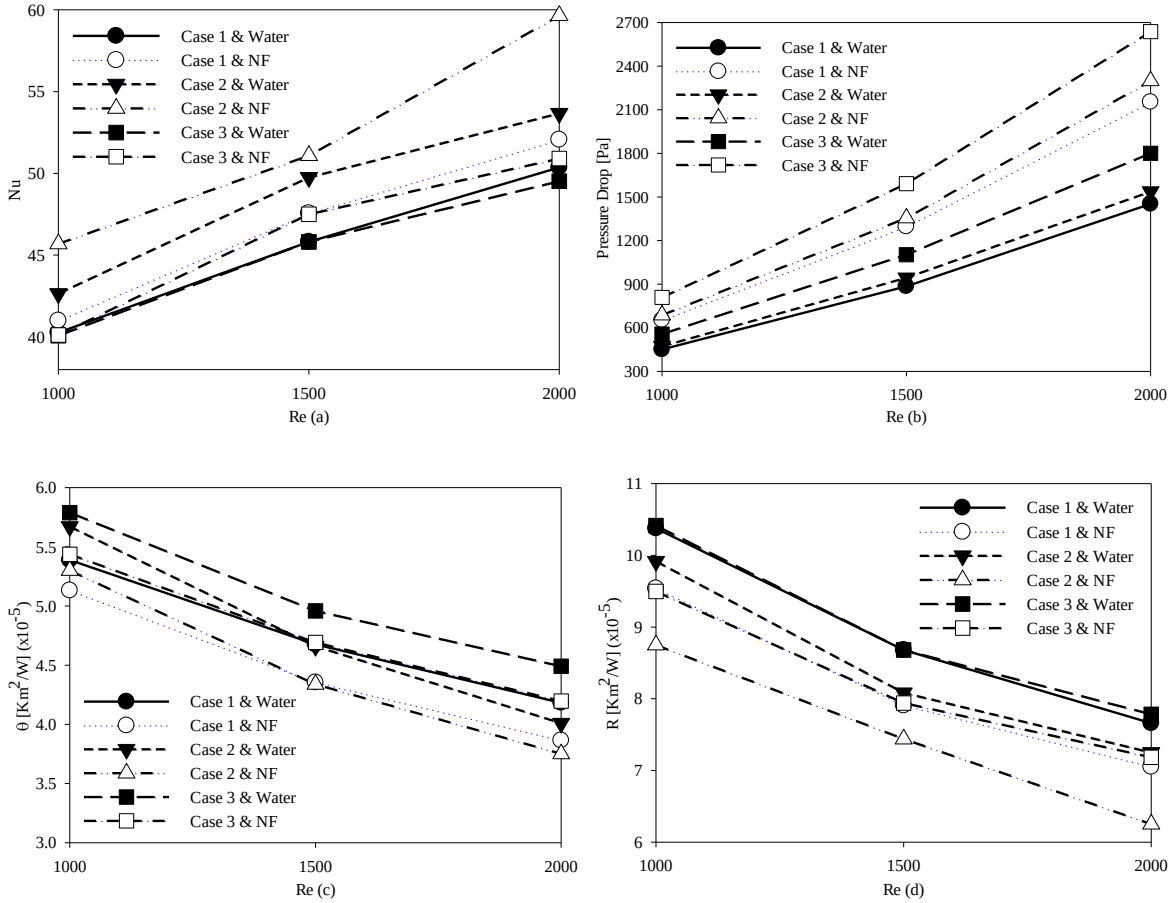

Fig. 3. Hydrothermal characteristics of the proposed system, a) Nu, b) Pressure drop, c) Temperature uniformity, d) Thermal resistance.

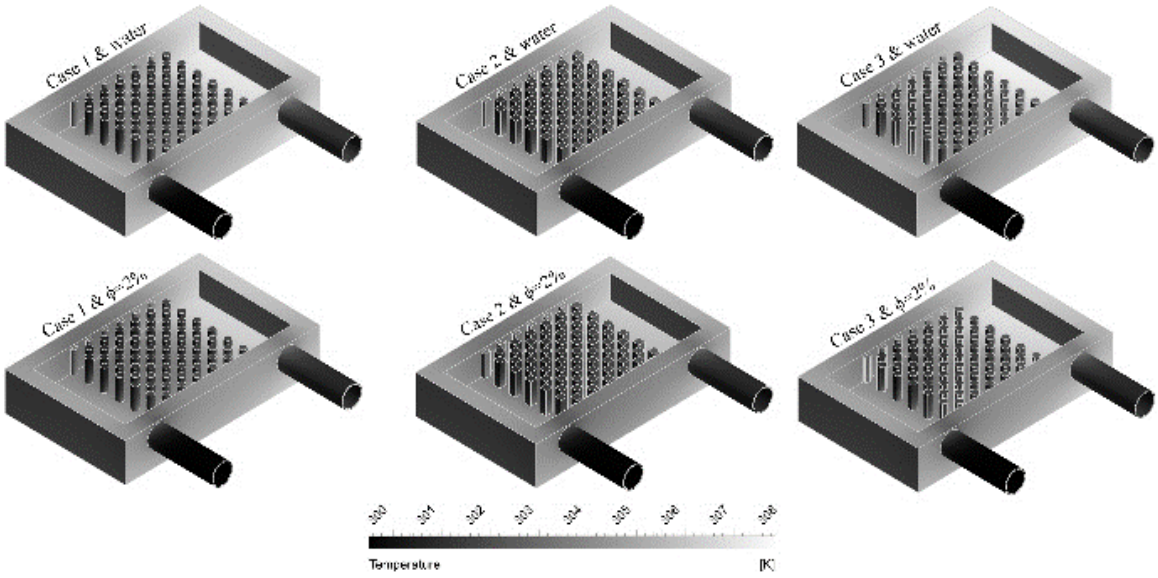

Fig. 4. Temperature distribution on heatsink for different fin designs at Re=2000 and φ=2%.

Fig. 4 presents temperature distribution for all cases at Re=2000. As can be seen in this figure, inlet section and finned area are cooler than outlet section. The reason of that the acceleration of fluid is higher in that region than outlet section. Also, in the finned section, cooler surface was obtained due to increasing in surface area. As can be seen from this figure, using of fin at the middle of the heatsink leads to less cooling efficiency a region which is close to outlet section. However, for overall efficiency, using of find inside heatsink is better approximation for cooler surfaces. Furthermore, Case 2 & NF with φ=2% shows the maximum efficiency in terms of cooling.

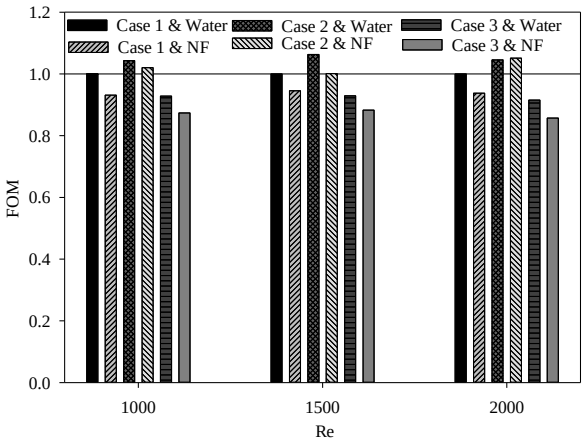

Fig. 5. Figure of merit (FOM) for all proposed design and working fluid parameters.

FOM defines applicability of proposed design considering all parameters. As can be seen in Fig. 5, the maximum FOM was handled using Case 2 & NF while the minimum one belongs to Case 3 & NF due to higher pressure drop value. The main negative parameter is the pressure drop for FOM that is why Case 3 presents lower FOM number than other proposals.

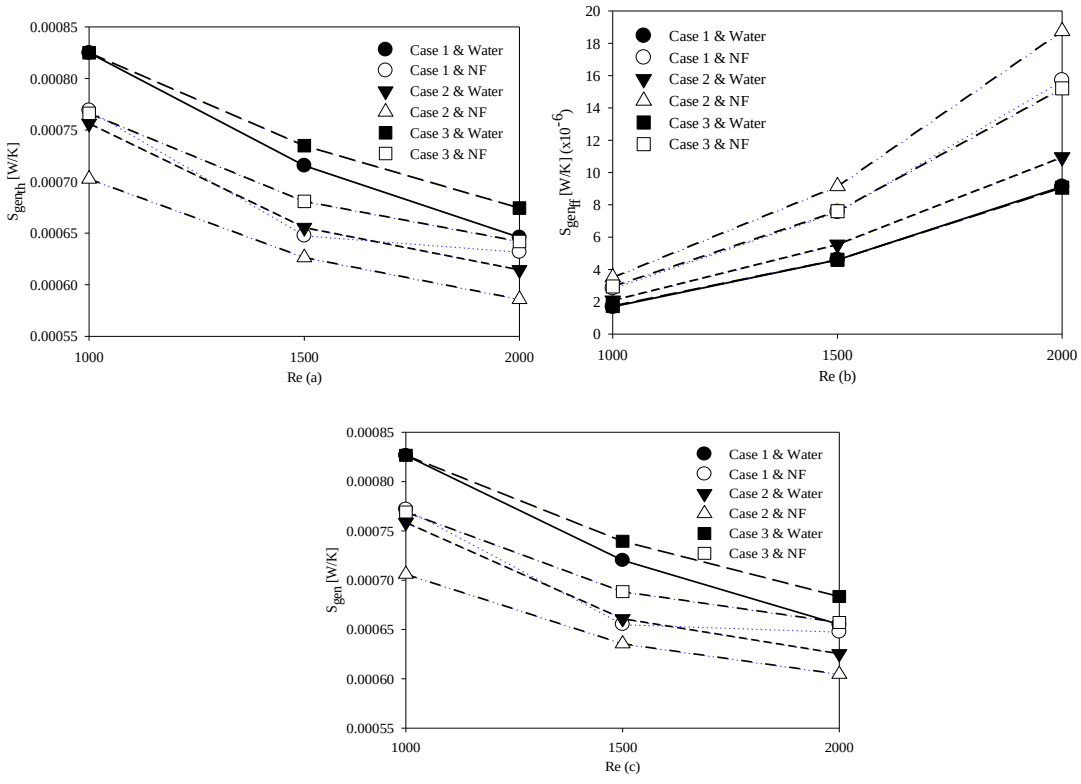

Fig. 6. Entropy generation due to a) thermal irreversibility, b) frictional irreversibility, c) total.

Fig. 6 (a, b, c) highlights entropy generation for all cases. Fig. 6a presents entropy generation in terms of thermal irreversibility. As can be seen from this figure, the use of NF affects positively in terms of thermal irreversibility. For example, the use of Case 3 & water presents the highest thermal irreversibility whilst Case 2 & NF gives the lowest one which is better in terms of entropy generation. It is known that using of nanofluids causes the higher thermal performance, so their capabilities on entropy generation is enhanced, so they lead to decrease in thermal entropy generation. In Fig. 6b denotes frictional irreversibility for all cases. The minimum one was obtained for Case 3 & water, and the maximum one was seen for Case 2 & NF. Overall, total entropy generation can be seen in Fig. 6c for all cases. The best one is Case 2 & NF in terms of total entropy generation.

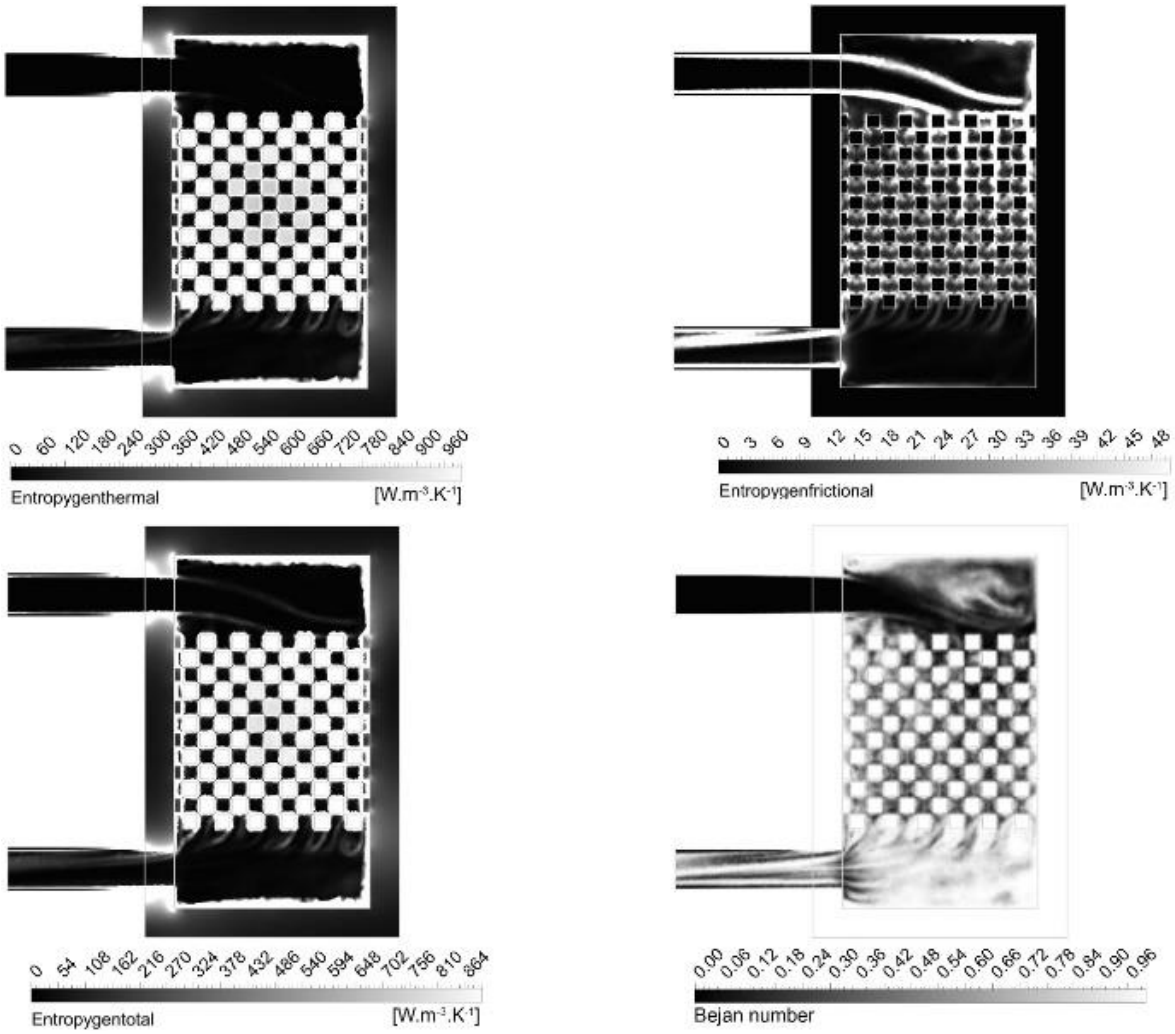

Fig. 7. Entropy generation in volume and Bejan number distribution for square pin finned heatsink at Re=2000 and φ=2%.

Fig. 7 (a, b, c, d) presents entropy generation contours for the best-case name Case 2 & NF. As can be seen from this figure, the maximum thermal entropy generation occurs heatsink's and fin boundaries due to the fact that Nu is higher in these areas than other zones. Also, the frictional entropy generation is higher at inlet section and fins boundaries due to the fact that pressure drop is the high in these areas. While total entropy generation is similar to thermal irreversibility since thermal entropy generation is dominant for this case. Bejan number is the lowest around the inlet section, but it is the higher toward fin and outlet section since the thermal irreversibility is higher at these regions.

IV. CONCLUSION

In this study, finned heatsink was extensively analysed in terms of first and second law of thermodynamics. Herein, 2 different working fluids and 3 different design parameters were determined for 3 Res(1000-1500-2000). The main findings of this study can be seen below:

1. The use of square pin fin inside heatsink is a satisfied approach for achieving a well-designed thermo hydraulic characteristics for removing heat from electronic devices.
2. The Nu was enhanced by 18.41% using Case 2 & NF compared to Case 1 & water at Re=2000 while pressure drop was dramatically increased around %59 for the same comparison at Re=1000.
3. FOM reached its best value at Re=1500 for Case 2 & water since FOM criticise both thermal achievements and hydraulic penalties.
4. Total entropy generation was obtained with its minimum value for Case 2 & NF for all Res.
5. Finally, Case 2 & NF was obtained as the best offer for both energy and entropy generation compared to other cases.

For future studies, the same pin fin arrangements should be designed for different size and placement zone to define optimum distances among pin fins and their number inside heat sink. Then, exergy efficiency, economical aspect, environmental issues should be taken into account for this study as well as energy and entropy generation.

NOMENCLATURE

D_h	Hydraulic Diameter [m]
ff	Friction factor
FOM	Figure of Merit
Nu	Average Nusselt Number
NF	Nanofluid
gen	Generation
th	Thermal
T	Temperature [K]
Re	Reynolds number
S	Entropy (W/K)
q”	Heat flux [W/m^2]
ρ	Density [kg/m^3]
μ	Dynamic viscosity [Pa.s]
φ	Nanoparticle volumetric concentration (%)

REFERENCES

Algburi, N. İ. H., Pazarlıoğlu, H. K., & Arslan, K. (2021). Effect of Pitch Ratio and Diagonal Length of Pin Fin of Heat Sink on Convective Heat Transfer for Turbulent Flow Condition. *Avrupa Bilim ve Teknoloji Dergisi*, *28*(28), 643–652. https://doi.org/10.31590/EJOSAT.1009980

Ateş, A., Çelik, S., Yağcı, V., Çağlar Malyemez, M., Parlak, M., Sadaghiani, A. K., & Koşar, A. (2023). Flow boiling of dielectric fluid HFE – 7000 in a minichannel with pin fin structured surfaces. *Applied Thermal Engineering*, *223*. https://doi.org/10.1016/j.applthermaleng.2023.120045

Ateş, A., Parizad Benam, B., Yağcı, V., Çağlar Malyemez, M., Parlak, M., Sadaghiani, A. K., & Koşar, A. (2022). On the effect of elliptical pin Fins, distribution pin Fins, and tip clearance on the performance of heat sinks in flow boiling. *Applied Thermal Engineering*, *212*. https://doi.org/10.1016/j.applthermaleng.2022.118648

Chen, L., Brakmann, R. G. A., Weigand, B., Poser, R., & Yang, Q. (2020). Detailed investigation of staggered jet impingement array cooling performance with cubic micro pin fin roughened target plate. *Applied Thermal Engineering*, *171*, 115095.

Ghazizade-Ahsaee, H., Shahsavar, A., Askari, I. B., & Damghani, H. (2023). The effect of inlet velocity profile on entropy generation and hydrothermal performance of a pin-fin heatsink with biologically prepared silver/water nanofluid coolant: Two-phase mixture model. *Engineering Analysis with Boundary Elements*, *150*, 309–317. https://doi.org/10.1016/j.enganabound.2023.02.026

Gürsoy, E., Pazarlıoğlu, H. K., Gürdal, M., Gedik, E., & Arslan, K. (2023). Entropy generation of ferronanofluid flow in industrially designed bended dimpled tube. *Thermal Science and Engineering Progress*, *37*, 101620. https://doi.org/10.1016/J.TSEP.2022.101620

Jiji, L. M. (2009). Heat convection: Second edition. *Heat Convection: Second Edition*, 1–543. https://doi.org/10.1007/978-3-642-02971-4

Kays, W. M., Crawford, M. E., & Weigand, B. (2004). *Convective heat and mass transfer* (4th ed., Vol. 4). Mcgraw-Hill (Tx).

Li, D., Zhuang, J., Liu, T., Lu, Z., & Zhou, S. (2011). The pressure loss and ribbon thickness prediction in gap controlled planar-flow casting process. Journal of Materials Processing Technology, 211(11), 1764-1767.

Parlak, M., Özsunar, A., & Koşar, A. (2022). High aspect ratio microchannel heat sink optimization under thermally developing flow conditions based on minimum power consumption. *Applied Thermal Engineering*, *201*. https://doi.org/10.1016/j.applthermaleng.2021.117700

Pazarlıoğlu, H. K., Ekiciler, R., & Arslan, K. (2021). Numerical Analysis of Effect of Impinging Jet on Cooling of Solar Air Heater with Longitudinal Fins. *Heat Transfer Research*, *52*(11), 47–61. https://doi.org/10.1615/HEATTRANSRES.2021037251

Pazarlıoğlu, H. K., Ekiciler, R., Arslan, K., & Adil Mohammed Mohammed, N. (2023a). Exergetic, Energetic, and entropy production evaluations of parabolic trough collector retrofitted with elliptical dimpled receiver tube filled with hybrid nanofluid. *Applied Thermal Engineering*, *223*, 120004. https://doi.org/10.1016/J.APPLTHERMALENG.2023.120004

Pazarlıoğlu, H. K., Gürsoy, E., Gürdal, M., Tekir, M., Gedik, E., Arslan, K., & Taşkesen, E. (2023b). The First and Second Law Analyses of Thermodynamics for CoFe2O4/H2O Flow in a Sudden Expansion Tube Inserted Elliptical Dimpled Fins. *International Journal of Mechanical Sciences*, 108144. https://doi.org/10.1016/J.IJMECSCI.2023.108144

Pazarlıoğlu, H. K., Tepe, A. Ü., & Arslan, K. (2022a). Optimization of Parameters Affecting Anti-Icing Performance on Wing Leading Edge of Aircraft. *European Journal of Science and Technology*, *34*(34), 19–27. https://doi.org/10.31590/EJOSAT.1062495

Pazarlıoğlu, H. K., Tepe, A. Ü., Tekir, M., & Arslan, K. (2022b). Effect of new design of elongated jet hole on thermal efficiency of solar air heater. *Thermal Science and Engineering Progress*, *36*, 101483. https://doi.org/10.1016/J.TSEP.2022.101483

Shahsavar, A., Ghazizade–Ahsaee, H., Baniasad Askari, I., & Setareh, M. (2023). Numerical feasibility study of using ultrasonic surface vibration as a new technique for thermal management of the electronic devices. *Energy Conversion and Management*, *276*. https://doi.org/10.1016/j.enconman.2022.116481

Shahsavar, A., Roohani, S., & Jahangiri, A. (2022a). Evaluation of the effect of rifled inlet on the hydrothermal performance and entropy generation of biological silver/water nanofluid-cooled heatsink. *Journal of Thermal Analysis and Calorimetry*, *147*(20), 11561–11575. https://doi.org/10.1007/s10973-022-11342-3

Shahsavar, A., Shahmohammadi, M., Arıcı, M., & Ali, H. M. (2022b). Extensive investigation of the fluid inlet/outlet position effects on the performance of micro pin-fin heatsink through simulation. *Energy Sources, Part A: Recovery, Utilization and Environmental Effects*, *44*(4), 9489–9505. https://doi.org/10.1080/15567036.2022.2134518

Shahsavar, A., Shahmohammadi, M., & Askari, I. B. (2021a). CFD simulation of the impact of tip clearance on the hydrothermal performance and entropy generation of a water-cooled pin-fin heat sink. *International Communications in Heat and Mass Transfer*, *126*. https://doi.org/10.1016/j.icheatmasstransfer.2021.105400

Shahsavar, A., Shahmohammadi, M., & Baniasad Askari, I. (2021b). The effect of inlet/outlet number and arrangement on hydrothermal behavior and entropy generation of the laminar water flow in a pin-fin heat sink. *International Communications in Heat and Mass Transfer*, *127*. https://doi.org/10.1016/j.icheatmasstransfer.2021.105500

Tekir, M., Gedik, E., Arslan, K., Pazarlıoğlu, H. K., Aksu, B., & Taskesen, E. (2022). Hydrothermal behavior of hybrid magnetite nanofluid flowing in a pipe under bi-directional magnetic field with different wave types. *Thermal Science and Engeering Progress*, *34*, 101399. https://doi.org/10.1016/J.TSEP.2022.101399